ChemComm

COMMUNICATION

View Article Online
View Journal | View Issue

Cite this: *Chem. Commun.*, 2015, 51, 10229

Received 23rd February 2015,
Accepted 14th May 2015

DOI: 10.1039/c5cc01621e

www.rsc.org/chemcomm

Highly sensitive turn-on biosensors by regulating fluorescent dye assembly on liposome surfaces†

Sungbaek Seo,‡[a] Min Sang Kwon,‡[b] Andrew W. Phillips,‡[a] Deokwon Seo[b] and Jinsang Kim*[abcde]

We developed a new self-signaling sensory system built on phospholipid liposomes having H-aggregated R6G dyes on their surface. Selective molecular recognition of a target by the phospholipid displaces R6G from the liposome surface to turn on fluorescence signal. Selective and sensitive detection of neomycin down to 2.3 nM is demonstrated.

Liposomes are spherical nanostructures consisting of a lipid bilayer surrounding an aqueous core. The unique bilayer architecture, dynamic nature, and functionalizable surface of liposomes provide an important scaffold for drug delivery[1] and for various analytical applications.[2] An attractive analytical application of liposomes is as a sensor platform for detecting important chemical and biological analytes.[3,4] Amplification of the sensory signal, good biocompatibility, and simple preparation without complex chemical synthesis of liposomes are attractive features for developing liposomes as a sensor platform.[5,6] Liposome-based sensors are typically composed of fluorescence dyes and/or electrochemical markers located in the aqueous core or within the lipid bilayer, with specific receptors conjugated onto the liposome surface.[7,8] When target analytes encounter the system, the receptors interact with the target analytes, thereby triggering the signal-generation mechanism through various signal transduction mechanisms such as liposome collapse, Förster resonance energy transfer (FRET), photoinduced electron transfer (PeT) between dyes and analytes or steric repulsion of analytes for affinochromic polymer liposomes.[9–15] However, dye encapsulation methods suffer from several drawbacks including low loading efficiency, poor control of the amount of encapsulated dyes, and self-quenching of dyes.

Herein, we report our systematic approach to develop a novel liposome-based sensing platform from the interesting observation: the fluorescence of Rhodamine 6G (R6G) dyes is efficiently quenched on phospholipid-liposome surfaces. Through thorough investigation of this observation, we revealed the origin of this phenomenon and developed a unique turn-on sensing platform able to detect bioanalytes, neomycin as an example, with very high sensitivity, down to 2.3 nM, one of the most sensitive aminoglycosidic antibiotic detection systems reported among liposome-based sensors.

We illustrated our strategy to realize the liposome-based sensing platform from the observation in Scheme 1. Liposome–R6G complexes used in the detection of target analytes were prepared from the mixed solution of phospholipids and polydiacetylene monomer (PCDA). Specific phospholipids were introduced to the system for selective interaction with target analytes and PCDA monomers are incorporated to enhance the stability of the liposome because PCDA can be photopolymerized. Coulombic interactions between

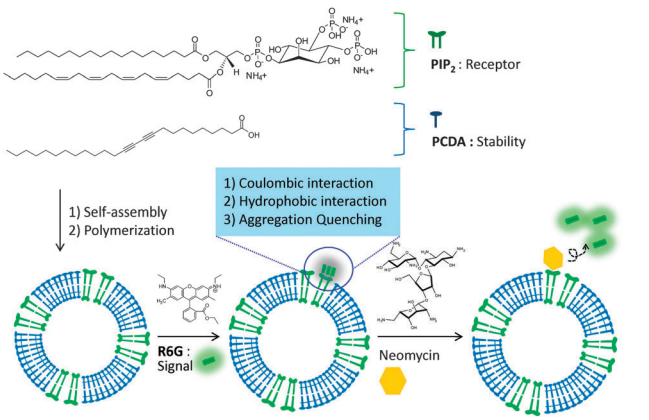

Scheme 1 Schematic illustration of the novel liposome-based turn-on sensor design principle. Diacetylene monomers (PCDA) and phospholipids are incorporated into the liposomes to enhance the stability of liposomes and to respond to target analytes, respectively. Rhodamine 6G (R6G) emission is quenched on the liposome surface by the formation of H-aggregates driven by Coulombic interactions between R6G dyes and phospholipids and concomitant hydrophobic interactions of dyes. Specific interaction between target analytes and phospholipids leads to the displacement of R6G dyes in favor of the target analytes, inducing the sensory signal.

[a] *Macromolecular Sci. and Eng., University of Michigan, USA*
[b] *Materials Sci. and Eng., University of Michigan, USA*
[c] *Chemical Eng., University of Michigan, USA*
[d] *Biomedical Eng., University of Michigan, USA*
[e] *Chemistry, University of Michigan, USA. E-mail: jinsang@umich.edu*

† Electronic supplementary information (ESI) available. See DOI: 10.1039/c5cc01621e

‡ S. Seo, M. S. Kwon, A. Phillips contributed equally to this work.

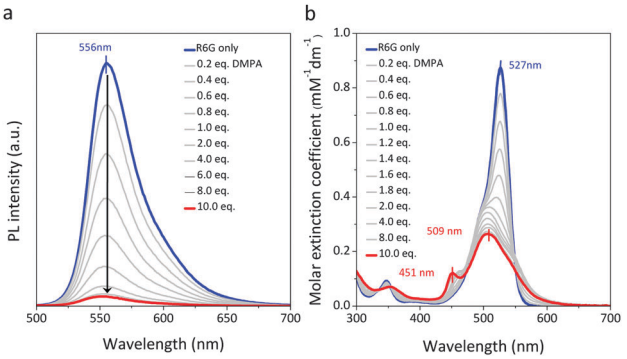

Fig. 1 (a) Photoluminescence (PL) spectra and (b) UV-Vis absorption spectra of R6G in the presence of DMPA.

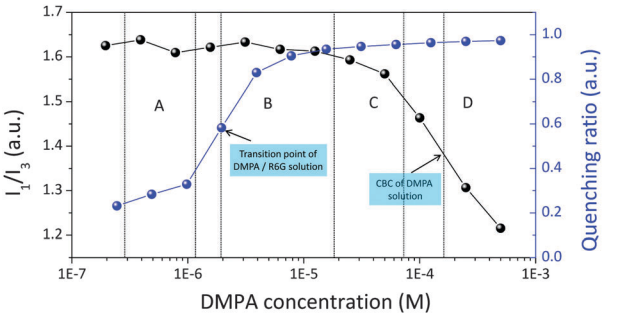

Scheme 2 Quenching ratio of R6G emission (blue circle) was plotted *versus* DMPA concentration. CBC value of DMPA was determined by I_1/I_3 value (black circle) using pyrene fluorescence probing (see Fig. S3 for details, ESI†).

cationic R6G dyes and anionic phospholipids and concomitant hydrophobic interactions of the resulting complexes caused aggregation-induced fluorescence quenching of R6G dyes on phospholipid-liposome surfaces. When the target analytes are added, strong specific interactions between phospholipids and the target analytes break the non-specific Coulombic interactions between R6G dyes and phospholipids, leading to displacement of R6G dyes by the target analytes and subsequent fluorescence recovery as a sensory signal.

When an aqueous solution of 1,2-dimyristoyl-*sn-glycero*-3-phosphate (DMPA; 1×10^{-4} M, 20 μl; a chemical structure in Fig. S1, ESI†) was added to an aqueous solution of R6G (1×10^{-5} M, 1 ml), the fluorescence of R6G was gradually quenched as the amount of DMPA increased (Fig. 1a). A dramatic change was also observed in the UV-Vis spectrum. The main absorption band at 527 nm progressively decreased and new peaks at around 509 nm and 451 nm appeared (Fig. 1b). We hypothesized that this interesting R6G quenching originated from the aggregation-induced emission quenching by means of the formation of H-type aggregates of R6G mediated by DMPA.[16]

We developed the hypothesis based on the structural features of DMPA and R6G. DMPA is a phospholipid comprised of a water-soluble anionic head and two long hydrophobic alkyl tails. Due to this amphiphilic nature, it can readily form liposomes in water above its critical bilayer concentration (CBC).[17] R6G is a moderately water-soluble cationic dye. We assumed that negatively-charged DMPA would attract cationic R6G, triggering aggregation to minimize surface energy of the resulting hydrophobic R6G–DMPA complexes (Fig. S1, ESI†). Several studies have demonstrated that electrostatic interactions between cationic dyes and negatively-charged colloids such as micelles,[18] vesicles,[19] clays,[20] silica,[21] and self assembled monolayer-treated gold nanoparticles,[22] led to aggregation of dye molecules, supporting our hypothesis.

We carefully compared three different amphiphilic molecules with different charge characteristics to confirm our hypothesis. Positively-charged hexadecyltrimethylammonium bromide (CTAB) and neutral polyoxyethylene (20) sorbitan monolaurate (Tween 20) did not show any signature for R6G aggregation, while negatively charged sodium lauryl sulfate (SDS) generated H-type aggregates of R6G dyes (Fig. S1, ESI†). These results clearly indicate that Coulombic interactions play a crucial role in R6G aggregation, as we expected. However, when KH_2PO_4 was added to a water solution of R6G, we did not observe R6G aggregation even though KH_2PO_4 has a negative charge on its own (Fig. S1, ESI†). We attribute this to the absence of long alkyl chains in KH_2PO_4. Even if KH_2PO_4–R6G complexes form *via* Coulombic interactions, it is difficult to assemble into aggregates because the resulting KH_2PO_4–R6G complexes are quite hydrophilic and stable enough in an aqueous environment.

We investigated the PL quenching ratio of R6G *versus* DMPA concentration to understand the detailed mechanism of R6G aggregation. The curve in Scheme 2 shows a transition point at a very low concentration, 0.002 mM; rapid quenching started from 0.001 mM and saturated at around 0.01 mM. SEM analysis combined with dynamic light scattering study indicates that R6G dyes and DMPA lipids assemble to form spherical nanoparticles, *i.e.* liposomes, above the CBC and this led to R6G aggregation as well (Fig. S2, ESI†). To determine CBC value of DMPA, fluorescence intensities of the peaks at ~375 nm (I_1) and ~385 nm (I_3) were extracted from the PL spectra (Fig. S3, ESI†). The I_1/I_3 values were plotted against the serially diluted lipid concentration; the inflection point of this plot is defined as CBC (Scheme 2).[23] Furthermore, the fact that the transition concentration (0.002 mM) of quenching ratio is far below the CBC of DMPA (~0.3 mM) implies that the DMPA–R6G complexes resulting from Coulombic interactions are more hydrophobic than pure DMPA and so the complexes can form liposomes even at much lower concentrations of DMPA than the CBC of DMPA. After obtaining a clear picture of the R6G aggregation mechanism through systematic analysis, we further investigated the strength of the Coulombic interactions between DMPA and R6G in an aqueous environment. We calculated the binding constant (K_b) through PL titration of an aqueous solution of DMPA with R6G (Fig. S4, ESI†). The K_b value was measured to be 6.3×10^5 in the presence of 0.1 equiv. of R6G, which is consistent with other reported systems and is strong enough to form DMPA–R6G complexes in water.[24] Interestingly, the measured K_b value decreased as the amount of R6G increased despite the fact that K_b value should be constant, theoretically, implying that R6G already bound to liposome surfaces may interfere with binding of other R6G dyes.

Based on the systematic analysis of this observation, we developed a new sensory platform to detect various bioanalytes. It is well known that phospholipids specifically interact with bioanalytes.[25]

We envisioned that the specific interaction between phospholipids and target analytes would break the non-covalent interactions between R6G and phospholipids leading to displacement of R6G dyes by the target analytes and subsequent fluorescence recovery as a fluorescence turn-on sensory signal.

Our initial trial to use R6G–DMPA liposomes as a sensory platform was unsuccessful because the liposomes easily precipitated out of solution in 1–2 days at room temperature (Fig. S5, ESI†). To achieve long-term stability and convenient preparation of the liposome solution, we decided to co-assemble diacetylene monomers, which are well-known to accommodate various phospholipids and form stable liposomes.[26,27] Co-assembled liposomes were expected to be easily polymerized by UV light, leading to the enhanced stability of the liposomes in solution. We prepared a co-assembled liposome solution comprised of DMPA–PCDA by following the reported procedure (Note: detailed procedure is also described in the experimental section).[26,27] Subsequent treatment of the co-assembled liposome solution with 254 nm UV-light resulted in polymerized liposomes as the developed blue color implies. As expected, the resulting liposome solution shows excellent stability without forming aggregation or precipitation for months under ambient conditions.

We examined whether the co-assembled liposomes can still induce the R6G quenching. Addition of R6G dyes into the liposome solution indeed resulted in significant emission quenching of the dyes, which is in accordance with the DMPA–R6G system. Changes in UV-Vis spectrum clearly indicate that R6G dyes form H-type R6G aggregates on the co-assembled liposome surfaces through Coulombic interactions. We calculated the K_b value for the co-assembled liposome through a PL titration (Fig. S6, ESI†). Very interestingly, the calculated K_b value was 3 times higher than for that of DMPA–R6G. We assumed that the well-regulated surface of co-assembled liposome would increase K_b value, but do not fully understand the increase in K_b value yet.

We selected neomycin as a target analyte. Neomycin is an aminoglycosidic antibiotic with diverse applications in human and veterinary medicine, particularly in the livestock industry. Due to the ototoxicity and nephrotoxicity of neomycin, there is interest in monitoring the levels of the drug in livestock products. Furthermore, overuse of neomycin contributes to antibiotic-resistant bacteria, providing another motivation to monitor levels of the drug in the food supply. Phosphatidylinositol 4,5-bisphosphate (PIP_2), a lipid component of cellular membranes, is part of the inositol 1,4,5-triphosphate/diacylglycerol signal transduction pathway. Normally, PIP_2 acts as a substrate for the enzyme phospholipase C, which catalyzes the hydrolysis of the lipid. Neomycin is known to bind PIP_2, which inhibits the hydrolysis, and thus the downstream signal cascade.[26]

We prepared an aqueous solution of polymerized co-assembled liposomes (Fig. S7, ESI†) comprised of PCDA : PIP_2 (1 : 1, 50 μM). Addition of R6G dye to the liposome solution resulted in significant emission quenching of the dye. The changes in the UV-Vis spectrum clearly indicate that the emission quenching of the dyes is attributed to the formation of H-type aggregates of R6G on liposome surfaces (Fig. 2a). We calculated the quenching efficiency of R6G dyes for the PIP_2–R6G complexes through UV-Vis titration. The maximum quenching of the PIP_2–R6G system was observed at 2.2 equivalents

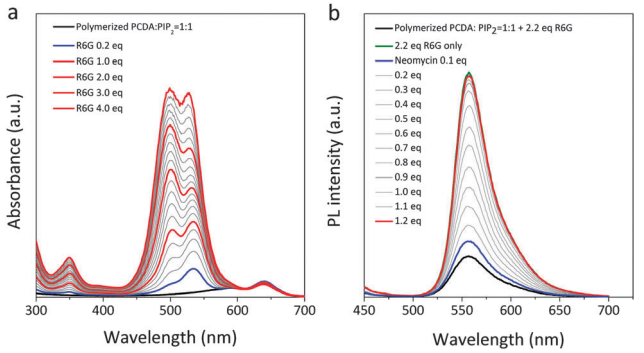

Fig. 2 (a) UV-Vis absorption spectra of PCDA–PIP_2 based liposomes in the presence of different amounts of R6G. (b) Changes in PL spectra of PCDA–PIP_2–R6G based liposome sensor by the addition of neomycin.

of R6G (Fig. 2a). The formation of H-type aggregates of dyes should theoretically reach the maximum quenching efficiency at 3.0 equivalents of dyes for the PIP_2–R6G system because PIP_2 contains three phosphate groups (refer the PIP_2 structure in Scheme 1). We attributed this difference to the structural features of PIP_2, which possesses two external phosphates and one internal phosphate group. The two outside phosphate groups can easily interact with R6G dyes and cause H-aggregates, while the internal phosphate may not able to bind efficiently with dyes due to the large steric hindrance. As shown in Fig. S8 (ESI†), addition of neomycin to the PCDA–PIP_2 liposome–R6G system restored the shape of the absorption spectra of R6G, but did not change the absorption of the photopolymerized PCDA at around 650 nm meaning that PCDA did not contribute to the optical transition of this sensor system. As the amount of neomycin increased, the emission intensity of R6G gradually increased and it restored the original fluorescence when 1.2 equivalents of neomycin were added (Fig. 2b), implying that neomycin forms a 1 : 1 complex with PIP_2, which is in good accordance with previous research.[28]

We conducted sensitivity tests with the DI-water solution of neomycin at various concentrations. Distinguishable R6G emission recovery was observed with 2.3 nM neomycin, which is at least 10 times better than the established 0.1 μM of detection limit of neomycin in our previously published system (Fig. 3a).[29] We stretched our detection

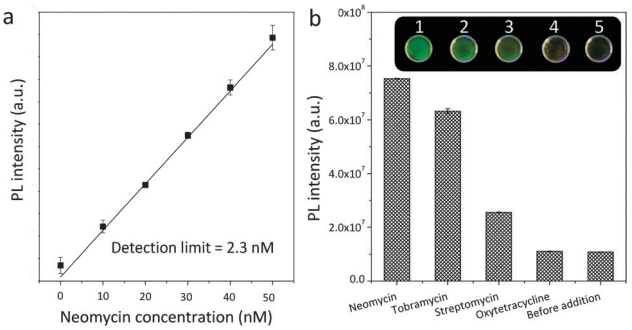

Fig. 3 (a) PL intensity of PCDA–PIP_2–R6G based liposome sensor was indicated *versus* neomycin concentration in the system. Black line shows linear fitting curve. (b) PL intensity of PCDA–PIP_2–R6G based liposome sensor was measured in the presence of the same concentration of neomycin (1), tobramycin (2), streptomycin (3), and oxytetracycline (4).

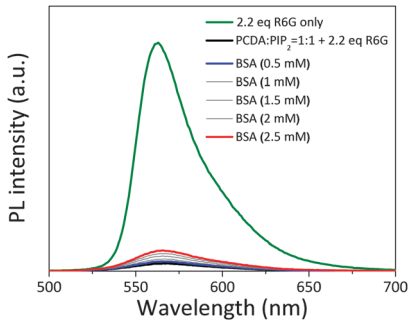

Fig. 4 Changes in PL spectra of PCDA–PIP_2–R6G liposome solution as various concentration of BSA is added.

study to other aminoglycosidic antibiotics (tobramycin, streptomycin) because PIP_2 lipids are known to bind to aminoglycosidic antibiotics including neomycin.[30,31] As predicted, the liposome sensor also generated a certain level of a fluorescence turn-on (Fig. 3b). The turn-on signal intensity for aminoglycosidic antibiotics showed a trend (neomycin > tobramycin > streptomycin), which is identical to interaction strength of aminoglycosidic antibiotics toward PIP_2 in our previous study.[26] However, non-aminoglycosidic antibiotic, *i.e.*, oxytetracycline, having a different chemical structure from the aminoglycosidic antibiotics, did not produce any sensory signals. Since the H-aggregation formation relies on the Coulombic interaction between the R6G and phospholipids, we were concerned that the physiological environment (high ionic strength) would induce the de-quenching of R6G dyes by a charge screening effect, resulting in decreased selectivity. Unfortunately, as we expected, the sensor system showed considerable de-quenching of dyes in PBS buffer condition. To address this matrix effect, we designed a sample-preparation procedure to remove interfering species by using dialysis membranes with molecular weight cut-offs higher than buffer species but lower than the analyte molecular weight. We showed that dialysis of PBS buffer significantly reduced the signal to manageable levels (Fig. S9, ESI†). Centrifugal desalting columns and microwell spin plates could alternatively be used for a faster and high-throughput sample pre-treatment process. We also conducted additional selectivity test with Bovine Serum Albumin (BSA) protein that contains cationic 59 lysine residues. However, BSA did not induce significant false signal even at very high concentrations (2.5 μM) compared to the detection limit (2.3 nM) of neomycin, indicating that our system has sufficient selectivity to be used as a sensory platform for real-life applications (Fig. 4). The presented sensory platform has several merits: high sensitivity, readily applicable to other sensor designs, and conveniently compatible with conventional 96-well plates and microplate readers used for ELISA.

We developed a novel liposome-based fluorescence turn-on sensing platform by assembling R6G to a H-type aggregation on phospholipid-liposome surfaces. Rationally devised displacement of the R6G aggregates at the phospholipid-liposome surface by target analytes driven by the specific interaction between receptors and analytes releases R6G dyes from the aggregates, producing a bright fluorescence turn-on signal. This new sensory platform can be readily applicable to other sensor designs and compatible with conventional 96-well plates and microplate readers for ELISA.

We acknowledge the financial support from Animal, Plant and Fisheries Quarantine and Inspection Agency of Korea (I-AD14-2011-13-11) and the Converging Research Center Program funded by the Ministry of Science, ICT and Future Planning (NRF-2014M3C1A8048791).

Notes and references

1 K. Raemdonck, K. Braeckmans, J. Demeester and S. C. De Smedt, *Chem. Soc. Rev.*, 2014, **43**, 444.
2 A. Jesorka and O. Orwar, *Annu. Rev. Anal. Chem.*, 2008, **1**, 801.
3 N. Dave and J. Liu, *Adv. Mater.*, 2011, **23**, 3182.
4 K. W. Y. Chan, G. Liu, X. Song, H. Kim, T. Yu, D. R. Arifin, A. A. Gilad, J. Hanes, P. Walczak, P. C. M. van Zijl, J. W. M. Bulte and M. T. McMahon, *Nat. Mater.*, 2013, **12**, 268.
5 K. A. Edwards and A. J. Baeumner, *Anal. Chem.*, 2007, **79**, 1806.
6 F. Patolsky, A. Lichtenstein and I. Willner, *J. Am. Chem. Soc.*, 2001, **123**, 5194.
7 J. Zhou, Q.-X. Wang and C.-Y. Zhang, *J. Am. Chem. Soc.*, 2013, **135**, 2056.
8 R. Gui, A. Wan, X. Liu and H. Jin, *Chem. Commun.*, 2014, **50**, 1546.
9 Y. Wang, K. Zhou, G. Huang, C. Hensley, X. Huang, X. Ma, T. Zhao, B. D. Sumer, R. J. DeBerardinis and J. Gao, *Nat. Mater.*, 2013, **13**, 204.
10 X. Chen, G. Zhou, X. Peng and J. Yoon, *Chem. Soc. Rev.*, 2012, **41**, 4610.
11 X. Sun, T. Chen, S. Huang, L. Li and H. Peng, *Chem. Soc. Rev.*, 2010, **39**, 4244.
12 D. J. Anh and J. M. Kim, *Acc. Chem. Res.*, 2008, **41**, 805.
13 S. Seo, J. Lee, E. J. Choi, E. J. Kim, J. Y. Song and J. Kim, *Macromol. Rapid Commun.*, 2013, **34**, 743.
14 J. Lee, H. J. Kim and J. Kim, *J. Am. Chem. Soc.*, 2008, **130**, 5010.
15 J. Lee, H. Jun and J. Kim, *Adv. Mater.*, 2009, **21**, 3674.
16 M. Ogawa, N. Kosaka, P. L. Choyke and H. Kobayashi, *ACS Chem. Biol.*, 2009, **4**, 535.
17 J. T. Buboltz and G. W. Feigenson, *Langmuir*, 2005, **21**, 6296.
18 V. K. Kelkar, B. S. Valalulikar, J. T. Kunjappu and C. Manohar, *Photochem. Photobiol.*, 1990, **52**, 717.
19 M. D. Deumie, P. Lorente and D. Morizon, *J. Photochem. Photobiol., A*, 1995, **89**, 239.
20 F. L. Arbeloa, M. J. T. Estevez, T. L. Arbeloa and I. L. Arbeloa, *Langmuir*, 1995, **11**, 3211.
21 C. Nasr, D. Liu, S. Hotchandani and P. V. Kamat, *J. Phys. Chem.*, 1996, **100**, 11054.
22 I. S. Lim, F. Goroleski, D. Mott, N. Kariuki, W. Ip, J. Luo and C. Zhong, *J. Phys. Chem. B*, 2006, **110**, 6673.
23 K. Kalyanasundaram and J. K. Thomas, *J. Am. Chem. Soc.*, 1977, **99**, 2039.
24 C.-C. You, O. R. Miranda, B. Gider, P. S. Ghosh, I.-B. Kim, B. Erdogan, S. A. Krovi, U. H. F. Bunz and V. M. Rotello, *Nat. Nanotechnol.*, 2007, **2**, 318.
25 B. Mu, J. Zhang, T. P. McNicholas, N. F. Reuel, S. Kruss and M. S. Strano, *Acc. Chem. Res.*, 2014, **47**, 979.
26 D. H. Kang, H.-S. Jung, N. Ahn, J. Lee, S. Seo, K.-Y. Suh, J. Kim and K. Kim, *Chem. Commun.*, 2012, **48**, 5313.
27 D. H. Kang, H.-S. Jung, J. Lee, S. Seo, J. Kim, K. Kim and K.-Y. Suh, *Langmuir*, 2012, **28**, 7551.
28 S. Nawaz, A. Kippert, A. S. Saab, H. B. Werner, T. Lang, K.-A. Nave and M. Simons, *J. Neurosci.*, 2009, **29**, 4794.
29 The limit of detection (LOD) calculated from $S/N = 3$ ratio was found to be 2.3 nM at concentration range from 10 nM to 50 nM. The original PL spectra were shown in Fig. S6 (ESI†).
30 L. A. A. Rooijen and B. W. Agranoff, *Neurochem. Res.*, 1985, **10**, 1019.
31 S. Au, N. D. Weiner and J. Schacht, *Biochim. Biophys. Acta, Biomembr.*, 1987, **902**, 80.

